Muscle & Nerve

WILEY

MUSCLE&NERVE

BASIC SCIENCE RESEARCH ARTICLE OPEN ACCESS

Cyclosporine A Delays the Terminal Disease Stage in the *Tfam* KO Mitochondrial Myopathy Mouse Model Without Improving Mitochondrial Energy Production

Benjamin Chatel[1] | Isabelle Varlet[1] | Augustin C. Ogier[2] | Emilie Pecchi[1] | Monique Bernard[1] | Julien Gondin[3] | Håkan Westerblad[4] | David Bendahan[1] | Charlotte Gineste[1]

[1]Aix-Marseille Univ, CNRS, CRMBM, Marseille, France | [2]Aix Marseille Univ, Université de Toulon, CNRS, Lis, Marseille, France | [3]Institut NeuroMyoGène, Unité Physiopathologie et Génétique du Neurone et du Muscle, UMR CNRS 5261—INSERM U1315, Université Claude Bernard Lyon 1, Lyon, France | [4]Department of Physiology and Pharmacology, Karolinska Institutet, Stockholm, Sweden

Correspondence: Charlotte Gineste (ginestec@igbmc.fr)

Received: 17 January 2024 | **Revised:** 28 November 2024 | **Accepted:** 1 December 2024

Funding: This work was supported by AFM-Téléthon (trampoline grant #19963 to CG). CRMBM is a member of the France Life Imaging network (grant ANR-11-INBS-0006).

Keywords: force production | mitochondrial function | muscle disease | pharmacological agent | preclinical model

ABSTRACT

Introduction and Aims: Mitochondrial myopathies are rare genetic disorders for which no effective treatment exists. We previously showed that the pharmacological cyclophilin inhibitor cyclosporine A (CsA) extends the lifespan of fast-twitch skeletal muscle-specific mitochondrial transcription factor A knockout (*Tfam* KO) mice, lacking the ability to transcribe mitochondrial DNA and displaying lethal mitochondrial myopathy. Our present aim was to assess whether the positive effect of CsA was associated with improved in vivo mitochondrial energy production.

Methods: Mice were treated with CsA for 4 weeks, beginning at 12 weeks (i.e., before the terminal disease phase). Hindlimb plantar flexor muscles were fatigued by 80 contractions (40 Hz, 1.5 s on, 6 s off) while measuring force and energy metabolism using phosphorus-31 magnetic resonance spectroscopy.

Results: Force decreased at similar rates in *Tfam* KO mice with and without the CsA treatment, reaching 50% of the baseline value after ~14 ± 1 contractions, which was faster than in control mice (25 ± 1 contractions). Phosphocreatine (PCr) decreased to ~10% of the control concentration in *Tfam* KO mice, independent of the treatment, which was larger than the ~20% observed in control mice. The time constant of PCr recovery was higher in untreated *Tfam* KO than that in control muscle (+100%) and similar in untreated and CsA-treated *Tfam* KO mice.

Discussion: The results do not support improved mitochondrial energy production as a mechanism underlying the prolonged lifespan of *Tfam* KO mitochondrial myopathy mice treated with CsA. Thus, other mechanisms must be involved, such as the previously observed CsA-mediated protection against excessive mitochondrial Ca^{2+} accumulation.

1 | Introduction

Mitochondrial myopathies comprise a heterogeneous group of genetic diseases often resulting in the failure to generate the required cellular energy by oxidative phosphorylation [1]. Patients with mitochondrial disease display a range of skeletal muscle-related clinical manifestations, including muscle wasting, weakness, and exercise intolerance [2–4]. No effective therapy is available and agents aimed at increasing respiratory chain components, ketogenic diet, amino acid supplementation, and

exercise are the main therapeutic options for alleviating the muscle symptoms [5–8]. Furthermore, the complex and variable phenotypes of mitochondrial myopathies make it difficult to assess treatment efficacy [9, 10].

Mice with fast-twitch skeletal muscle-specific deletion of the gene for mitochondrial transcription factor A (*Tfam* KO mice) faithfully reproduce the main structural and clinical muscle features of mitochondrial myopathy, that is, atrophy, ragged red fibers, weakness, decreased endurance, and mitochondrial dysfunction [11, 12]. At an age of ~3 months, *Tfam* KO mice enter a stage of decay, which is manifested as rapidly developing weight loss and muscle weakness, and death occurs ~1 month afterward [13]. We recently showed impaired mitochondrial energy production and premature fatigue development before *Tfam* KO mice enter the terminal stage with rapidly developing weight loss and muscle weakness [11]. These results agree with previous data obtained in mouse models with mitochondrial dysfunction, as well as in patients with mitochondrial myopathies [14–16]. In addition, an abnormally large and slowly reversible increase in mitochondrial Ca^{2+} was observed during repeated contractions in *Tfam* KO muscle fibers and this was suggested to play a major role in the disease process [17]. The excessive mitochondrial Ca^{2+} uptake was partially inhibited by cyclosporine A (CsA) [17]. CsA is a pharmacological agent that binds to the mitochondrial matrix protein peptidyl-prolyl cis-trans isomerase F (also known as cyclophilin D, CypD) and is considered to desensitize the opening of the mitochondrial permeability transition pore [18]. Interestingly, the protein expression of CypD was increased in *Tfam* KO muscles and also in patients with mitochondrial myopathies [13], thus implying that treatment with CsA might be effective in combating muscle defects in these myopathies. Consistent with this, the CsA treatment counteracted the rapidly progressing terminal muscle weakness and extended the lifespan of *Tfam* KO mice [13]. Likewise, a novel, specific cyclophilin inhibitor, NV556, was recently found to limit the excessive mitochondrial Ca^{2+} uptake and prolong the lifespan of *Tfam* KO mice [13]. The positive effects of treating *Tfam* KO mice with CsA involved protection against a decreased sarcoplasmic reticulum Ca^{2+} release, and hence a reduced force production, whereas it did not prevent a marked decrease in protein expression of the mitochondrial DNA-encoded cytochrome oxidase subunit 1 [13]. This implies that mitochondrial myopathies might be effectively treated with pharmacological agents that do not improve mitochondrial respiration. However, this counterintuitive implication clearly requires further investigation.

Thus, the aim of the present study was to assess whether CsA treatment affected in vivo muscle fatigue development and mitochondrial energy production in *Tfam* KO mice.

2 | Methods

2.1 | Animals, Groups, and Treatment

Male and female *Tfam* KO mice and control littermates (referred to as wild-type, WT) were used for experiments. The fast-twitch skeletal muscle-specific *Tfam* KO mouse model was generated as previously described [12]. *Tfam* KO and WT mice were randomly assigned to either the treated or untreated group. Treated mice received CsA as previously described [13], that is, 120 μg/day for 4 weeks via osmotic pumps (Alzet, micro-osmotic pump, Model 1004) implanted subcutaneously on the back under anesthesia (2.5% isoflurane in 33% O_2 and 66% NO_2). CsA treatment started when mice were ~12 weeks old. Untreated WT and *Tfam* KO mice had pump implantation with vehicle (i.e., containing only saline: 2 of 15 *Tfam* KO mice; 4 of 11 WT mice). Other untreated mice were left without pumps. No sex-related body weight progression was observed for either treatment. Therefore, males and females were pooled together. In addition, we did not observe any effects of the pump implantation or CsA treatment in WT mice (Figures S1 and S2). Thus, pooled mean data from CsA-treated and untreated WT mice were used for comparison with results obtained in *Tfam* KO mice. Different colors and/or symbols were used for individual data points from mice with or without pump implantation and with placebo or CsA.

All experiments were conducted in agreement with the French guidelines for animal care and in accordance with the European Convention for the Protection of Vertebrate Animals used for Experimental and other Scientific Purposes, and institutional guidelines n°86/609/CEE November 24, 1986. All animal experiments were approved by the Institutional Animal Care Committee of Aix-Marseille University (permit number #12522–2017121119249655 v1). Mice were housed in an environment-controlled facility (12–12 h light–dark cycle at 22°C) and received water and standard food *ad libitum*.

2.2 | Experimental Design

The body weight was measured every 2 to 3 days. Mice were subjected to strictly noninvasive in vivo anatomical and functional measurements in muscles of the left hindlimb. These experiments were performed at an age of 16 weeks or earlier if mice started to lose weight, that is, before they reached > 20% of body weight loss. The contractile performance of plantar flexor muscles (*gastrocnemius* [Gas], *soleus* [Sol], and *plantaris*) was assessed by measuring the maximal tetanic force in the unfatigued state and the force produced during fatiguing stimulation (see below). Metabolic changes were evaluated before, during, and after fatiguing stimulation using phosphorus-31 magnetic resonance spectroscopy (^{31}P-MRS). Before the fatiguing protocol, the volume of hindlimb muscles was quantified by magnetic resonance imaging (MRI). At the end of the in vivo experiments, hindlimb muscles (Gas, Sol, *tibialis anterior* [TA], and *extensor digitorum longus* [EDL]) were harvested and weighed. Mice were euthanized by cervical dislocation.

2.3 | Force and Magnetic Resonance Measurements

Mice were initially anesthetized in an induction chamber (4% isoflurane in 33% O_2 (0.5 L/min) and 66% NO_2 (1 L/min)) and then placed supine in a custom-made cradle designed for strictly noninvasive functional investigation of left hindlimb

muscles. A custom-built facemask was used to maintain anesthesia throughout the experiment (1.75% isoflurane in 33% O_2 (0.2 L/min) and 66% NO_2 (0.4 L/min)). The hindlimb was centered inside a ^{1}H imaging coil and the belly of the gastrocnemius muscle was located above a ^{31}P-MRS surface coil. The foot was positioned at 90° flexion of the ankle joint on the pedal of a custom-made ergometer coupled to a force transducer. The analog electrical signal from the force transducer was amplified with a home-built amplifier (Operational amplifier AD620; Analog Devices, Norwood, MA, USA) and converted to a digital signal, which was monitored and recorded on a personal computer using the Powerlab 35/series system (AD Instruments, Oxford, United Kingdom). Muscle contractions were elicited by noninvasive transcutaneous electrical square-wave pulses (0.5 ms duration) delivered via two rod-shaped surface electrodes integrated into the cradle and connected to an electrical stimulator (Digitimer Ltd., Model DS7A, Welwyn Springs, UK). The electrodes were placed on the left hindlimb, one at the heel level and the other immediately above the knee joint. The electrical current required to obtain maximal muscle activation was individually determined by progressively increasing the pulse amplitude until there was no further increase in peak twitch force. A 150 Hz tetanic stimulation train with a duration of 0.75 s was used to assess the maximal tetanic force of the plantar flexor muscles in the unfatigued state. Force production of the plantar flexor muscles was also measured during a fatigue protocol consisting of 80 contractions at 40 Hz, 1.5 s on—6 s off [11, 19].

MR experiments were performed using a 47/30 Biospec Avance MR system (Bruker, Karlsruhe, Germany) equipped with a 120-mm BGA12SL (200 mT/m) gradient insert. Anatomical MRI data were acquired at rest, that is, before functional measurements. Fifteen consecutive contiguous axial slices (thickness = 0.7 mm), covering the region from the knee to the ankle, were selected across the lower hindlimb. Rapid acquisition with relaxation enhancement (RARE) images (RARE factor = 4, effective echo time = 22.5 ms, actual echo time = 10.6 ms, repetition time = 1000 ms, number of averages = 10, number of repetitions = 1, field of view = 4.2 × 4.2 cm, matrix size = 256 × 192, and acquisition time = 8 min 00 s) were recorded. ^{31}P spectra (8-kHz sweep width; 2048 data points) from the posterior hindlimb muscle region were acquired continuously throughout the standardized rest-fatigue-recovery protocol. A total of 800 partially saturated (repetition time = 2 s) free induction decays (FID) were recorded.

2.4 | Data Processing

2.4.1 | Anatomical Imaging

MR images were analyzed using FSLview (FMRIB, Oxford, UK) [20]. The border of the whole hindlimb muscle area was manually delineated in the two slices located on the proximal and distal parts. Segmentations of the missing intermediate slices were automatically performed on the basis of registration procedures as described previously [21]. The volume of the hindlimb muscles (mm^3) was calculated as the sum of the volume of the 10 consecutive largest slices.

2.4.2 | Contractile Performance

The peak force of each contraction was measured using the LabChart software (AD Instruments, Oxford, United Kingdom). The specific force was expressed as the peak force (in mN) divided by the muscle volume (in mm^3; obtained from MR images). Force production during fatiguing stimulation is presented as the average of every 5 contractions and the sum of each individual peak force during the fatiguing stimulation. The C_{50} corresponds to the contraction number at which the force was decreased to 50% of the maximal force recorded during the fatigue protocol.

2.4.3 | Energy Metabolism

^{31}P-MRS data were processed using a proprietary software developed using IDL (Interactive Data Language, Research System Inc. Boulder, CO, USA) [22]. The first 180 FIDs were acquired at rest and summed together ($n = 1$, time resolution = 6 min). The next 320 FIDs were acquired during the stimulation period and summed by blocks of 80 ($n = 4$, time resolution = 160 s). The last 300 FIDs were acquired during the recovery period and summed by blocks of 50 ($n = 6$, time resolution = 100 s). The relative concentrations of the phosphate metabolites phosphocreatine (PCr) and inorganic phosphate (Pi) were obtained by a time-domain fitting routine using the AMARES-MRUI Fortran code and appropriate prior knowledge of the ATP multiplets. In order to correct for potential movement artifacts during fatiguing stimulation, Pi values were normalized to the sum of PCr and Pi values, which were considered to remain constant [23]. Intracellular pH (pH_i) was calculated from the chemical shift of the Pi signal relative to the PCr signal [24]. The resting phosphocreatine to ATP ratio was calculated from the peak areas of the phosphocreatine and β-ATP of the spectrum acquired at rest. Changes during the fatiguing protocol (ΔPCr, maximal Pi/(Pi+PCr), ΔpH_i) and the post-fatiguing recovery period (PCr recovery time constant (τ_{PCr}), $[PCr]_{end\ recovery}$, $Pi/(Pi+PCr)_{end\ recovery}$) were extracted from the time-courses of PCr, Pi, and pH_i [11].

2.5 | Statistical Analysis

Data are presented as individual data points and mean ± SEM for bar graphs and as mean ± SEM for curves. Statistical analyses were performed using GraphPad Prism software version 9.1.2. Normality was checked using a Shapiro–Wilk test. Two-way ANOVA with repeated measures on contraction or time was used to assess differences in force production and metabolic changes during the induction of fatigue and the subsequent recovery period, respectively. Tukey's or Sidak's posthoc test was performed when a significant interaction was found. One-way ANOVA or Kruskal-Wallis test was used for normally and not normally distributed data, respectively, to compare WT, untreated *Tfam* KO, and CsA-treated *Tfam* KO groups. Tukey's post hoc test or Dunn's post hoc test was performed when a significant difference was observed. Unpaired t-test or Mann–Whitney test was used for normally and not normally distributed data, respectively, to compare untreated WT and CsA-treated WT. Statistical significance was accepted when $p < 0.05$.

3 | Results

3.1 | CsA Treatment Did Not Affect Anatomy, Contractile Function, or Metabolism in WT Mice

Four weeks of CsA treatment of WT mice had no significant effect on body weight, muscle volume, maximal tetanic force, or the force produced during fatiguing stimulation (Figure S1). Likewise, the CsA treatment did not significantly affect ^{31}P-MRS measurements of metabolites during the induction of fatigue and the subsequent recovery period in WT mice (Figure S2).

3.2 | CsA Treatment Delayed the Decline in Body Weight in *Tfam* KO Mice

Body weight of *Tfam* KO and WT mice was similar from an age of 10 weeks (*Tfam* KO 21 ± 1 g vs. WT 22 ± 1 g; $p > 0.05$) until the in vivo experiments were performed at 12 weeks (*Tfam* KO 20 ± 1 g vs. WT 20 ± 1 g; $p > 0.05$) (Figure 1A). Untreated *Tfam* KO mice started to lose weight after the intervention period was initiated: 1-week postintervention their weight was decreased by 3% ± 2% and only one mouse had not reached the ethical endpoint of 20% maximum of weight loss at 4 weeks after the start of

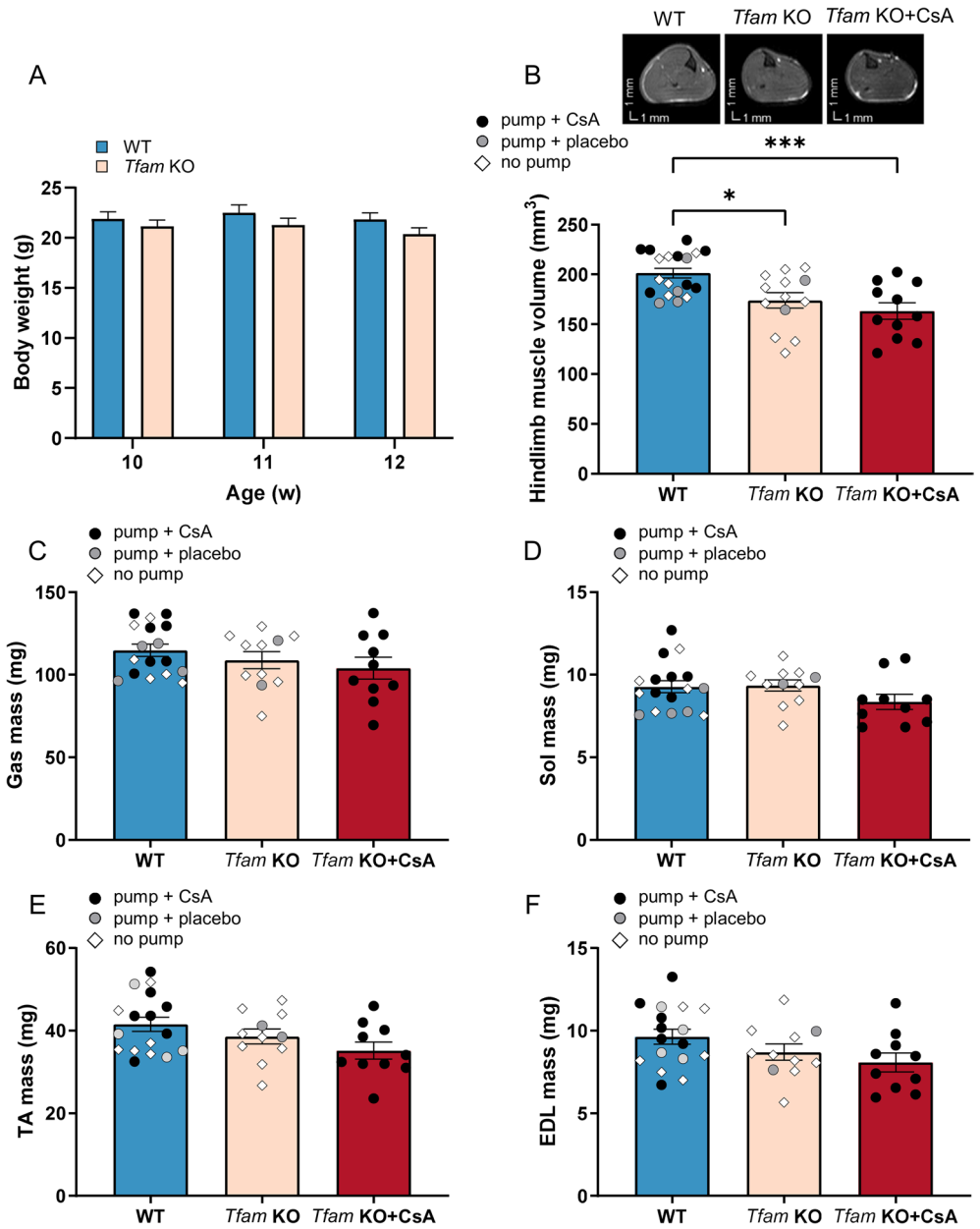

FIGURE 1 | Body weight was stable in *Tfam* KO mice during the CsA treatment period. (A) Body weight before the treatment period start. (B) Body weight during the treatment period. (C) Representative axial MR images obtained from untreated WT mice, untreated *Tfam* KO mice and CsA-treated *Tfam* KO mice (left panel), and quantification of the volume of hindlimb muscles in untreated and CsA-treated WT and *Tfam* KO mice (right panel). Mass of Gas (D), Sol (E), TA (F) and EDL (G). Data presented as individual values and mean ± SEM. *p*-values obtained with mixed-effects analysis with Sidak's post hoc test (panel A), mixed-effects analysis with Tukey's post hoc test (panel B), one-way ANOVA with Tukey's post hoc test (panel C–G). Significant difference *, ** and *** $p < 0.05$, 0.01 and 0.001, respectively.

the intervention. Consequently, in vivo experiments of untreated *Tfam* KO mice were performed at an age of ~14 weeks (i.e., before they reached the ethical endpoint). Conversely, CsA-treated *Tfam* KO mice had stable body weight throughout the 4 weeks of treatment ($p > 0.05$; 103% 2 weeks post-intervention and 99% 4 weeks post-intervention). Thus, no CsA-treated *Tfam* KO mice reached the ethical endpoint so they were tested at an age of ~16 weeks.

Hindlimb muscle volume was similarly decreased in CsA-treated and untreated *Tfam* KO mice as compared to WT mice (~15%; $p < 0.05$; Figure 1B). The mass of hindlimb muscles (Gas, Sol, TA, and EDL) was not significantly different between groups (Figure 1C–F).

3.3 | CsA Treatment Did Not Affect Maximal Force or Fatigue Development

The specific maximal tetanic (150 Hz) force in the unfatigued state was similar in WT, CsA-treated, and untreated *Tfam* KO mice (Figure 2A).

The decline in force production during fatiguing stimulation was similar in CsA-treated and untreated *Tfam* KO mice, and markedly faster than in WT mice (Figure 2B). Accordingly, the overall force produced during the stimulation protocol and the C_{50} (number of contractions at which force was 50% of the initial) were not different in CsA-treated and untreated *Tfam* KO mice and significantly lower than in WT mice (Figure 2C,D).

3.4 | Metabolites at Rest, During Repeated Contractions, and During Recovery Did Not Differ Between CsA-Treated and Untreated *Tfam* KO Mice

At rest ^{31}P-MRS measurements showed lower phosphocreatine (PCr) to ATP ratio (although not statistically significant in the untreated *Tfam* KO group), higher concentration of Pi (expressed as the Pi/(Pi + PCr) ratio), and lower pH_i in *Tfam* KO than in WT mice (Figure 3).

During fatiguing stimulation, the extent of PCr depletion was larger and Pi reached a higher level in *Tfam* KO than in WT mice (Figure 4A,B,D,E). On the other hand, the fatigue-induced

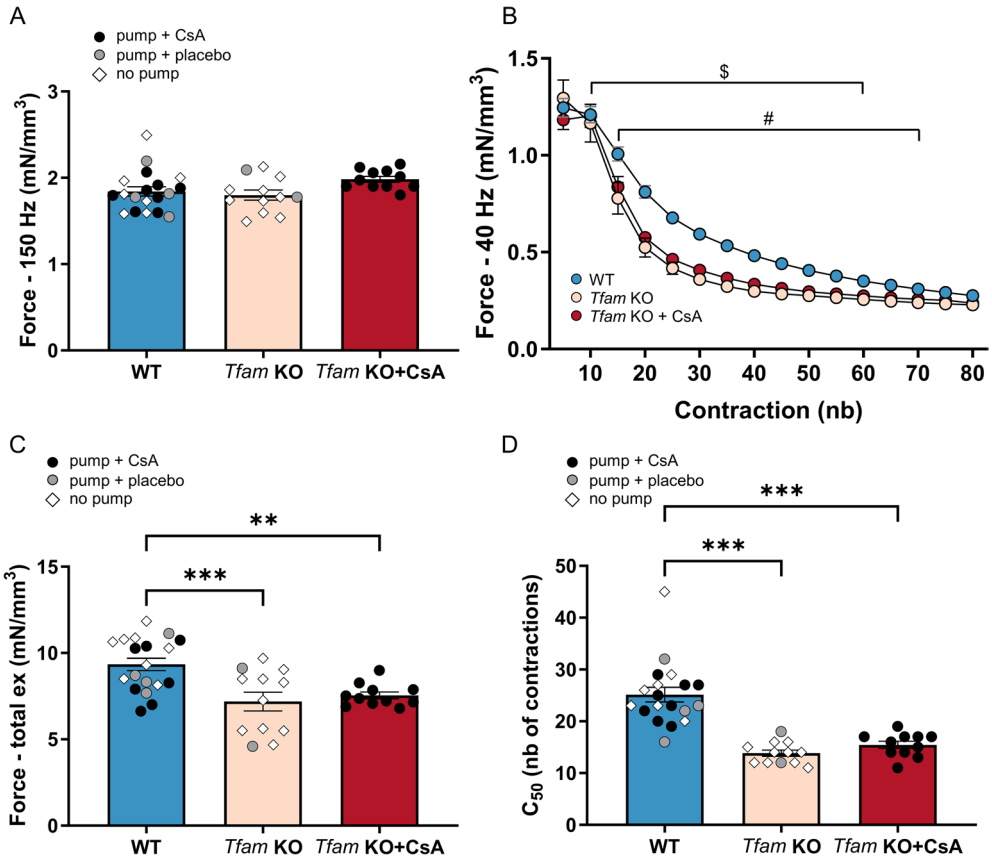

FIGURE 2 | CsA treatment did not affect maximal force in the unfatigued state or force decline during fatiguing stimulation. (A) Maximal (150 Hz) specific force (i.e., force divided by muscle volume) of the plantar flexor muscles in vivo. (B) In vivo specific force (i.e., force divided by muscle volume) of the plantar flexor muscles during fatigue induced by 80 contractions (40 Hz, 1.5 s on—6 s off). (C) Total specific force during the complete fatiguing protocol. (D) Contraction at which force production was 50% of the initial unfatigued force (C_{50}). Data presented as individual values and mean ± SEM for panels A, C, and D. Data presented as mean ± SEM for panel B. *p*-values obtained with one-way ANOVA with Tukey's posthoc test (panels A and C) or Kruskal-Wallis (panel D). Two-way ANOVA with repeated measures on contraction number with Tukey's posthoc test (panel B). Significant difference ** and *** $p < 0.01$ and 0.001, respectively. Significant difference WT versus *Tfam* KO $^{\#}$ $p < 0.05$. Significant difference WT versus *Tfam* KO + CsA $^{\$}$ $p < 0.05$.

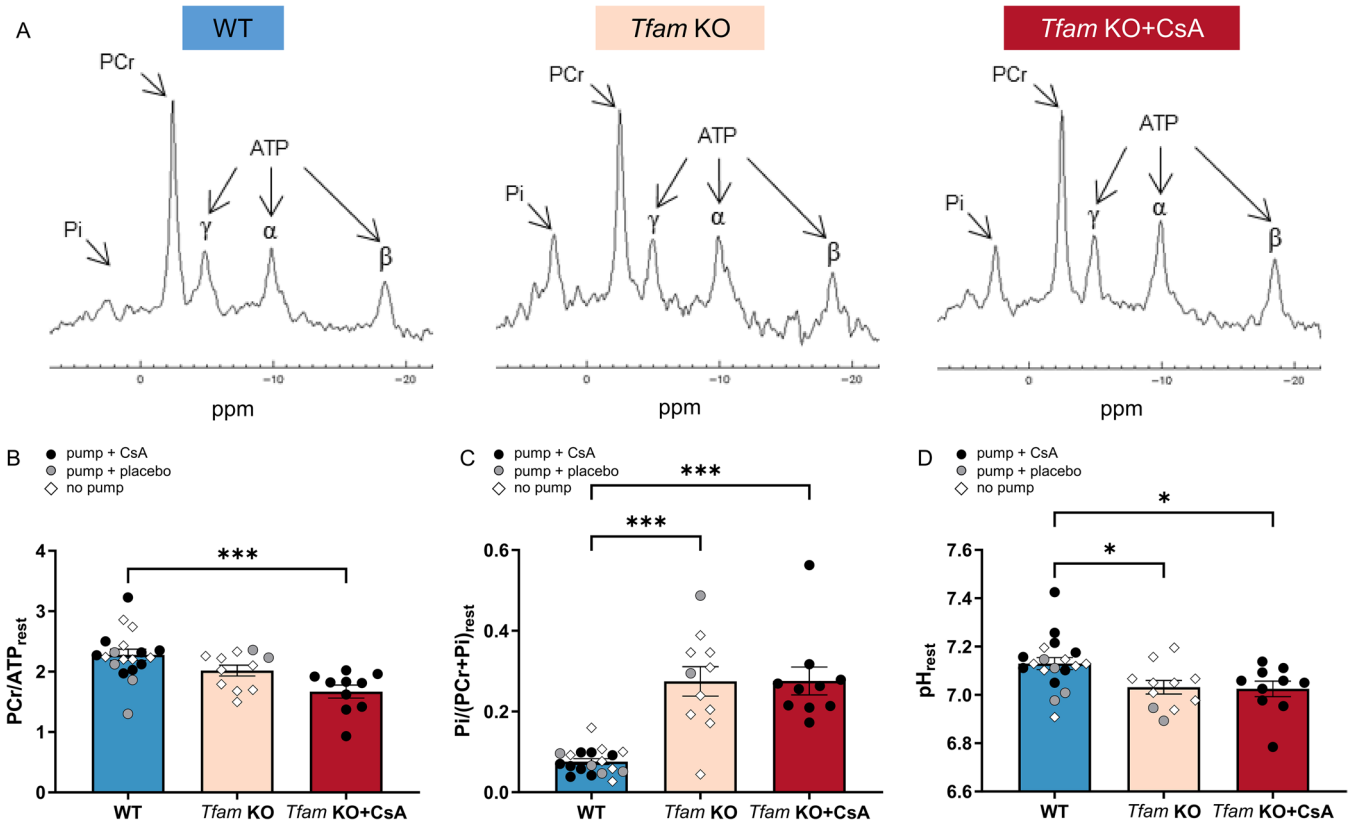

FIGURE 3 | Metabolic parameters at rest in the gastrocnemius muscle are unchanged following CsA administration. (A) Representative examples of resting ^{31}P-MR spectra in muscles of untreated WT mouse (left panel), untreated *Tfam* KO mouse (middle panel), and CsA-treated *Tfam* KO mouse (right panel). Data presented as individual values and mean ± SEM. *p*-values were obtained with one-way ANOVA with Tukey's posthoc test (panels B and D) or Kruskal-Wallis test with Dunn's posthoc test (panel C). Significant difference * and ***$p < 0.05$ and $p < 0.001$, respectively.

decline in pH_i was less marked in *Tfam* KO than in WT mice (Figure 4C,F). Notably, none of the measured metabolic changes during fatiguing stimulation showed any difference between CsA-treated and untreated *Tfam* KO mice.

After the fatiguing stimulation, the rate and total extent of PCr recovery were lower in *Tfam* KO than in WT mice (Figure 4G,H). CsA treatment of *Tfam* KO mice did not result in any marked difference in the measured PCr recovery parameters as compared to untreated *Tfam* KO mice. At the end of the 10 min recovery period, Pi had returned to the pre-fatigue resting values with higher Pi levels in *Tfam* KO than in WT mice (Figure 4I).

4 | Discussion

Our present findings confirm and extend previous results showing that pharmacological cyclophilin inhibition with CsA or NV556 postpones muscle weakness and body weight loss of *Tfam* KO mice, which takes place when these mice are about to enter the terminal myopathy phase [13, 25]. Intriguingly, our results imply that this beneficial effect of CsA treatment occurs despite no obvious improvement of the compromised mitochondrial energy production.

The present results demonstrate no effect of CsA treatment on the rate of force decline during fatiguing stimulation or changes in metabolites during the induction of fatigue and recovery in *Tfam* KO muscles. Our in vivo contraction experiments were performed at an early myopathy stage at which significant muscle weakness or muscle atrophy had not yet developed. Thus, fatigue resistance and energy metabolism were not affected by differences in muscle size or force production between untreated and CsA-treated mice. It was essential to perform the in vivo experiments before the development of muscle weakness because impairments in fatigue resistance and mitochondrial energy production might be masked by decreased specific force levels during fatiguing stimulation and hence reduced energy consumption. Indeed, we previously reported that the decrease in relative force during fatigue induced by repeated tetanic stimulation was similar in isolated fast-twitch EDL muscle and single fibers of flexor digitorum brevis (FDB) muscle of *Tfam* KO and littermate control mice [12, 17]. These experiments were performed in the terminal myopathy stage with the unfatigued force being 40% lower in isolated EDL and 25% lower in FDB single fibers in *Tfam* KO than in control muscles. Impaired SR Ca^{2+} release led to a reduction in unfatigued force; consequently, the rate of force decline during fatiguing stimulation was decreased by markedly reducing the energy consumption of cross-bridges and SR Ca^{2+} pumps [26]. Here, although in vivo fatiguing stimulation was performed earlier in the myopathy process where the unfatigued specific force was not yet decreased, force fell more rapidly in *Tfam* KO than in control muscles during in vivo fatiguing stimulation, as previously reported [11]. Nevertheless, CsA administration did

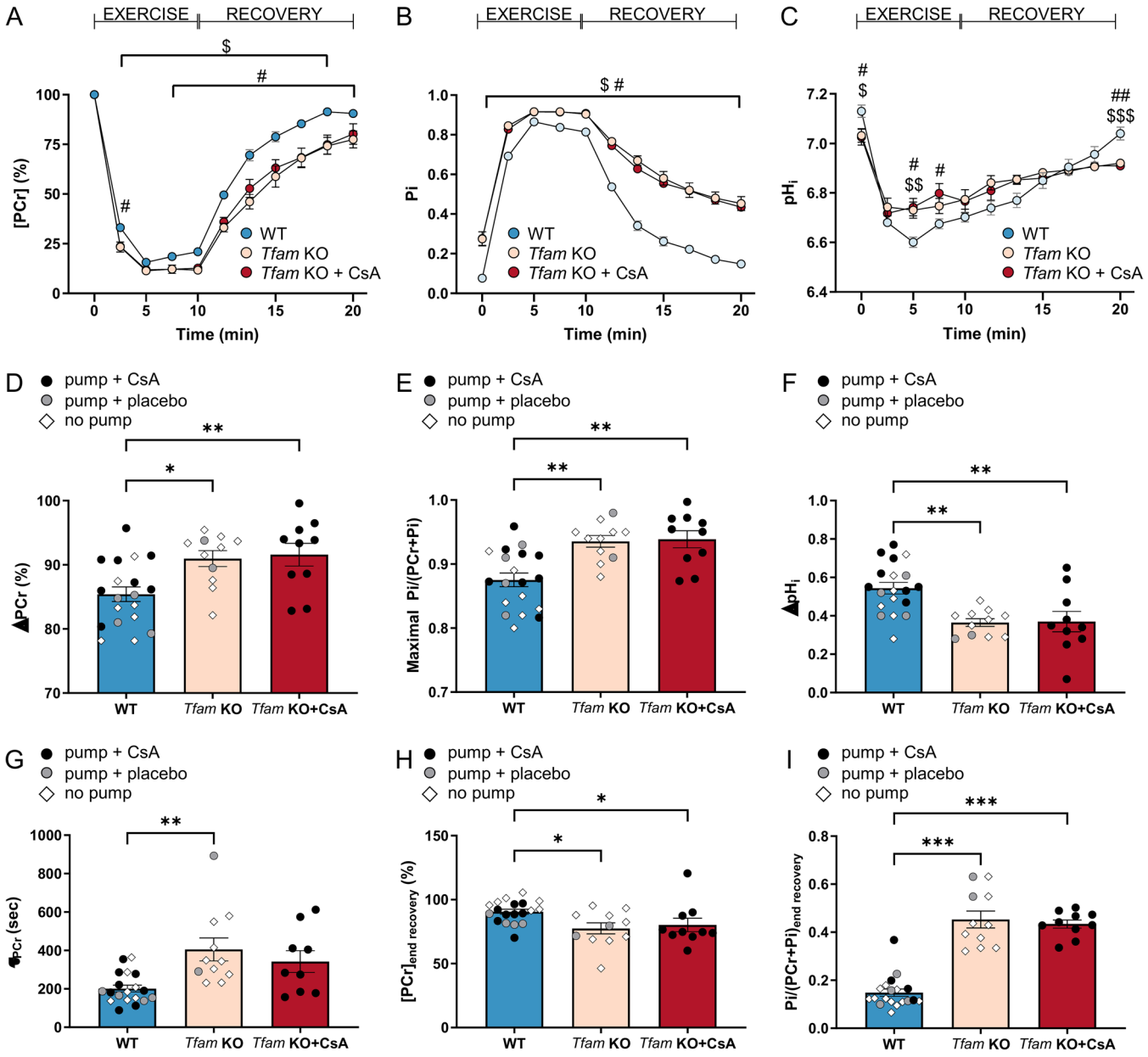

FIGURE 4 | CsA treatment had no effect on muscle metabolites during fatiguing stimulation and the following recovery. Levels of PCr (A), Pi (B), and pH_i (C) during the stimulation and recovery periods. Drop in PCr (D), maximal increase in Pi (E) and pH_i drop (F) during exercise. (G) Time constant of PCr recovery during the 10 min recovery phase after exercise. PCr (H) and Pi (I) at the end of the 10 min recovery period. Data presented as individual values and mean ± SEM for panels A–C. Data presented as mean ± SEM for panels D–I. *p*-values obtained with one-way ANOVA with Tukey's posthoc test (panels D–F) or Kruskal-Wallis test with Dunn's posthoc test (panels G–I). Significant difference *, ** and *** $p < 0.05$, 0.01 and 0.001, respectively. Two-way ANOVA with repeated measures on time and Tukey's post hoc test for PCr and Pi time-course and mixed-effects analysis with repeated measures on time and Tukey's posthoc test for pH_i. Significant difference WT versus *Tfam* KO $^{\#}$ and $^{\#\#}$ $p < 0.05$ and $p < 0.01$, respectively. Significant difference WT versus *Tfam* KO + CsA $^{\$}$, $^{\$\$}$ and $^{\$\$\$}$ $p < 0.05$, $p < 0.01$ and $p < 0.001$, respectively.

not counteract the faster fatigue development in *Tfam* KO than in control muscles. Muscle fatigue in *Tfam* KO mice was associated with larger changes and slower recovery of PCr and Pi. These data agree with previous results and imply impaired mitochondrial energy production in *Tfam* KO muscles before and immediately after the onset of the terminal myopathy stage [11]. PCr recovery kinetics, which are related to the end-exercise rate of oxidative ATP synthesis, are commonly used as a marker of oxidative mitochondrial capacity. Typically, an impaired mitochondrial oxidative function has been associated with a slower post-stimulation PCr recovery [27]. In *Tfam* KO mice, the rate of phosphocreatine recovery was strongly reduced and this impairment was not affected by CsA administration. Therefore, CsA treatment had no beneficial impact on mitochondrial energy production in *Tfam* KO muscles, which may account for the absence of muscle fatigue improvement following the CsA administration in *Tfam* KO mice. Our result fits with previous results showing no CsA-mediated protection against the marked decrease in protein expression of the mitochondrial DNA-encoded cytochrome oxidase subunit 1 [13].

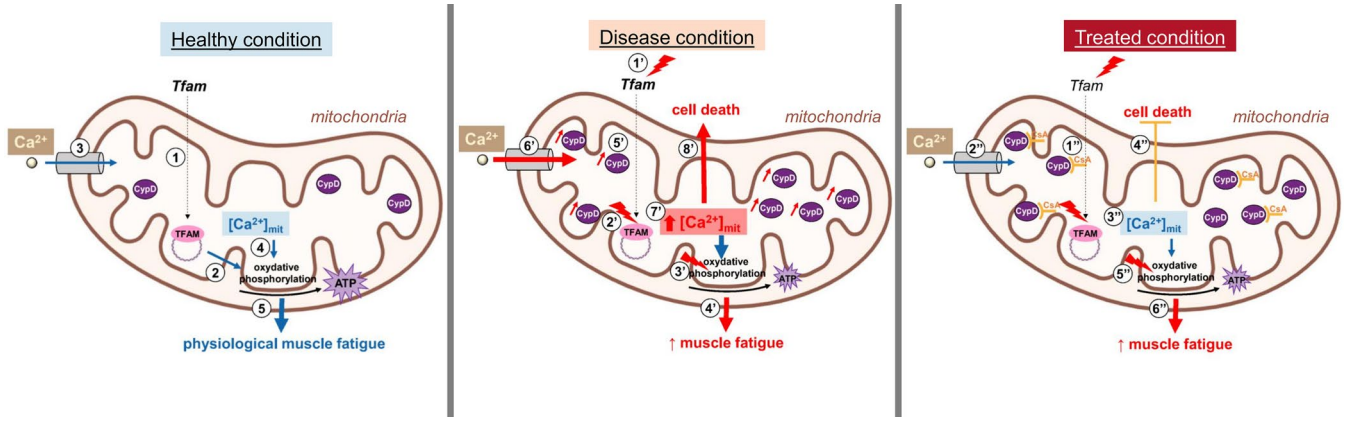

FIGURE 5 | Diagram representing proposed CsA mechanism of action in *Tfam* KO muscle. In healthy conditions (left panel), mitochondrial transcription factor A (TFAM) promotes mtDNA genome expression (1), encoding for 13 protein subunits of the electron transport chain (2) whereas mitochondrial Ca^{2+} entry (3) is required to stimulate ATP production by oxidative phosphorylation (4). Both TFAM and mitochondrial $[Ca^{2+}]$ are the main players in force maintenance during endurance exercise (5). In disease condition (middle panel), *Tfam* gene deletion (1′) causes a reduction in mtDNA maintenance and expression (2′) resulting in defective respiratory chain activity (3′) and increased muscle fatigue (4′). Maladaptive mechanisms to counteract impaired energy production, such as cyclophilin D (CypD)-dependent mitochondrial Ca^{2+} accumulation (5′ and 6′) to stimulate oxydative phosphorylation, leads in turn to excessive $[Ca^{2+}]$ (7′) which triggers cell death (8′). In the treated condition (right panel), cyclosporine A (CsA) inhibits CypD (1″), which limits Ca^{2+} entry into mitochondria (2″) resulting in physiological $[Ca^{2+}]$ (3″) and cell death prevention (4″). Oxidative phosphorylation is still defective due to altered electron transport chain activity (5″) leading to abnormally high muscle fatigue (6″). Blue arrow = positive effect. Red arrow = negative effect. Red flash = alteration. Orange line = positive effect of treatment. The figure was partly created with BioRender.com.

Weight loss has been shown to precede the decrease in unfatigued specific force in *Tfam* KO muscle [11]. The in vivo experiments on untreated *Tfam* KO mice were therefore performed as soon as these mice started to lose weight, which occurred at an age of ~14 weeks. On the other hand, CsA-treated mice needed to be followed beyond 14 weeks to ensure that the treatment was effective in delaying the disease process. The body weight of CsA-treated mice remained stable throughout the 4 weeks of treatment and hence these mice were tested at an age of ~16 weeks. Thus, the CsA-treated mice were older at the time of testing and we cannot exclude a further decline in mitochondrial energy production between 14 and 16 weeks that might have been prevented by CsA treatment.

Our results are consistent with those from a recently described mouse model with impaired mitochondrial function due to skeletal muscle-specific deletion of nicotinamide phosphoribosyltransferase (NAMPT) in which CsA treatment improved survival without affecting the energetic stress [28]. The protein expression of CypD was found to be increased in muscles of *Tfam* KO mice and patients with mitochondrial DNA depletion or mutations [13], as well as in the muscle-specific *Nampt*-deficient mouse model [28]. Marked positive effects of treatment with CsA as well as other cyclophilin inhibitors and genetic ablation of CypD have been observed in several mouse disease models of muscular dystrophy in which defective mitochondrial function is a key feature [28–32]. In addition, positive effects of CsA treatment have been reported in patients with CypD-dependent mitochondrial defects due to collagen VI mutations [33]. The protective effects of CypD inhibitors in muscular dystrophies were related to the maintenance of physiological Ca^{2+} homeostasis by improving mitochondrial abnormalities. CsA and the novel, specific cyclophilin inhibitor, NV556 limited the excessive mitochondrial Ca^{2+} uptake in muscle fibers of *Tfam* KO mice and prolonged their lifespans [17, 25]. Thus, the major mechanism underlying the positive effects of CypD inhibition in *Tfam* KO mice appears to be protection against deleterious effects of excessive and prolonged mitochondrial Ca^{2+} accumulation, rather than a direct effect on mitochondrial energy production.

Based on the present and previous results obtained with *Tfam* KO mice, we propose a model for the progression of mitochondrial myopathy and the beneficial effects of CsA treatment (Figure 5):

- A primary mitochondrial defect results in impaired energy production that triggers adaptations to counteract the deficiency and premature fatigue [11]. These adaptations include augmented CypD-dependent mitochondrial Ca^{2+} accumulation [13].
- In contrast to transient increases in mitochondrial Ca^{2+} that stimulate mitochondrial respiration, excessive and prolonged mitochondrial Ca^{2+} accumulation activates deleterious apoptotic and necrotic signaling [34–36], which results in weight loss, muscle wasting and weakness, and ultimately premature death.
- Pharmacological inhibition or genetic ablation of CypD hinders mitochondrial Ca^{2+} uptake and thereby prevents deleterious effects triggered by excessive and prolonged mitochondrial Ca^{2+} accumulation [13, 28–33].
- An impaired fatigue resistance remained following CypD inhibition, which implies no beneficial effect on the reduced oxidative phosphorylation caused by defective proteins of the electron transport chain.

In conclusion, 4 weeks of CsA administration delayed the progression into the terminal disease stage in *Tfam* KO mice, which implies that pharmacological CypD inhibitors have the potential to prevent the disease progression in patients with mitochondrial myopathies. Our results show that the positive effects of CsA treatment occurred despite no beneficial effects on mitochondrial energy production or fatigue development. Thus, other mechanisms must be involved, such as the previously observed CsA-mediated protection against excessive mitochondrial Ca^{2+} accumulation.

Author Contributions

Benjamin Chatel: investigation, writing – original draft, formal analysis. **Isabelle Varlet:** investigation. **Augustin C. Ogier:** methodology. **Emilie Pecchi:** investigation. **Monique Bernard:** writing – review and editing. **Julien Gondin:** writing – review and editing. **Håkan Westerblad:** writing – original draft, writing – review and editing. **David Bendahan:** writing – review and editing, supervision. **Charlotte Gineste:** conceptualization, funding acquisition, writing – original draft, writing – review and editing, formal analysis, supervision.

Acknowledgments

This work was funded by the AFM-Téléthon (trampoline grant #19963 to CG). CRMBM is a member of the France Life Imaging network (grant ANR-11-INBS-0006).

Ethics Statement

We confirm that we have read the Journal's position on issues involved in ethical publication and affirm that this report is consistent with those guidelines.

Conflicts of Interest

The authors declare no conflicts of interest.

Data Availability Statement

The authors confirm that the data supporting the findings of this study are available within the article and the Supporting Information. The data presented in this study are available on request from the corresponding author.

References

1. D. R. Thorburn, "Mitochondrial Disorders: Prevalence, Myths and Advances," *Journal of Inherited Metabolic Disease* 27, no. 3 (2004): 349–362.

2. R. K. Petty, A. E. Harding, and J. A. Morgan-Hughes, "The Clinical Features of Mitochondrial Myopathy," *Brain* 109, no. 5 (1986): 915–938.

3. T. Taivassalo, T. D. Jensen, N. Kennaway, S. DiMauro, J. Vissing, and R. G. Haller, "The Spectrum of Exercise Tolerance in Mitochondrial Myopathies: A Study of 40 Patients," *Brain* 126, no. 2 (2003): 413–423.

4. S. T. Ahmed, L. Craven, O. M. Russell, D. M. Turnbull, and A. E. Vincent, "Diagnosis and Treatment of Mitochondrial Myopathies," *Neurotherapeutics* 15, no. 4 (2018): 943–953.

5. T. Taivassalo and R. G. Haller, "Exercise and Training in Mitochondrial Myopathies," *Medicine and Science in Sports and Exercise* 37, no. 12 (2005): 2094–2101.

6. S. Ahola-Erkkila, C. J. Carroll, K. Peltola-Mjosund, et al., "Ketogenic Diet Slows Down Mitochondrial Myopathy Progression in Mice," *Human Molecular Genetics* 19, no. 10 (2010): 1974–1984.

7. D. Bendahan, C. Desnuelle, D. Vanuxem, et al., "^{31}P NMR Spectroscopy and Ergometer Exercise Test as Evidence for Muscle Oxidative Performance Improvement With Coenzyme Q in Mitochondrial Myopathies," *Neurology* 42, no. 6 (1992): 1203–1208.

8. J. F. Al, Z. N. Al, K. Al-Thihli, et al., "Endothelial Dysfunction and the Effect of Arginine and Citrulline Supplementation in Children and Adolescents With Mitochondrial Diseases," *Journal of Central Nervous System Disease* 12 (2020): 1179573520909377.

9. G. Pfeffer, R. Horvath, T. Klopstock, et al., "New Treatments for Mitochondrial Disease-No Time to Drop our Standards," *Nature Reviews. Neurology* 9, no. 8 (2013): 474–481.

10. H. Zweers, A. M. J. van Wegberg, M. C. H. Janssen, and S. B. Wortmann, "Ketogenic Diet for Mitochondrial Disease: A Systematic Review on Efficacy and Safety," *Orphanet Journal of Rare Diseases* 16, no. 1 (2021): 295.

11. B. Chatel, S. Ducreux, Z. Harhous, et al., "Impaired Aerobic Capacity and Premature Fatigue Preceding Muscle Weakness in the Skeletal Muscle *Tfam* KO Mouse Model," *Disease Models & Mechanisms* 14, no. 9 (2021): dmm048981.

12. A. Wredenberg, R. Wibom, H. Wilhelmsson, et al., "Increased Mitochondrial Mass in Mitochondrial Myopathy Mice," *Proceedings of the National Academy of Sciences* 99, no. 23 (2002): 15066–15071.

13. C. Gineste, A. Hernandez, N. Ivarsson, et al., "Cyclophilin D, a Target for Counteracting Skeletal Muscle Dysfunction in Mitochondrial Myopathy," *Human Molecular Genetics* 24, no. 23 (2015): 6580–6587.

14. T. Yamada, N. Ivarsson, A. Hernandez, et al., "Impaired Mitochondrial Respiration and Decreased Fatigue Resistance Followed by Severe Muscle Weakness in Skeletal Muscle of Mitochondrial DNA Mutator Mice," *Journal of Physiology* 590, no. 23 (2012): 6187–6197.

15. J. Finsterer, "Update Review About Metabolic Myopathies," *Lifestyles* 10, no. 4 (2020): 43.

16. M. A. Tarnopolsky, "Metabolic Myopathies," *CONTINUUM: Lifelong Learning in Neurology* 22, no. 6 (2016): 1829–1851.

17. J. Aydin, D. C. Andersson, S. L. Hanninen, et al., "Increased Mitochondrial Ca^{2+} and Decreased Sarcoplasmic Reticulum Ca^{2+} in Mitochondrial Myopathy," *Human Molecular Genetics* 18, no. 2 (2009): 278–288.

18. T. Briston, D. L. Selwood, G. Szabadkai, and M. R. Duchen, "Mitochondrial Permeability Transition: A Molecular Lesion With Multiple Drug Targets," *Trends in Pharmacological Sciences* 40, no. 1 (2019): 50–70.

19. C. Gineste, A. C. Ogier, I. Varlet, et al., "In Vivo Characterization of Skeletal Muscle Function in Nebulin-Deficient Mice," *Muscle & Nerve* 61, no. 3 (2020): 416–424.

20. M. Jenkinson, C. F. Beckmann, T. E. Behrens, M. W. Woolrich, and S. M. Smith, "Fsl," *NeuroImage* 62, no. 2 (2012): 782–790.

21. A. C. Ogier, L. Heskamp, C. P. Michel, et al., "A Novel Segmentation Framework Dedicated to the Followup of Fat Infiltration in Individual Muscles of Patients with Neuromuscular Disorders," *Magnetic Resonance in Medicine* 83, no. 5 (2020): 1825–1836.

22. Y. Le Fur, F. Nicoli, M. Guye, et al., "Grid-Free Interactive and Automated Data Processing for MR Chemical Shift Imaging Data," *Magma* 23, no. 1 (2010): 23–30.

23. B. Chance, S. Eleff, J. S. Leigh, Jr., D. Sokolow, and A. Sapega, "Mitochondrial Regulation of Phosphocreatine/Inorganic Phosphate Ratios in Exercising Human Muscle: A Gated 31P NMR Study," *Proceedings of the National Academy of Sciences* 78, no. 11 (1981): 6714–6718.

24. R. B. Moon and J. H. Richards, "Determination of Intracellular pH by ^{31}P Magnetic Resonance," *Journal of Biological Chemistry* 248, no. 20 (1973): 7276–7278.

25. C. Gineste, S. Youhanna, S. U. Vorrink, et al., "Enzymatically Dissociated Muscle Fibers Display Rapid Dedifferentiation and Impaired Mitochondrial Calcium Control," *Iscience* 25, no. 12 (2022): 105654.

26. A. J. Cheng, D. T. Hwee, L. H. Kim, et al., "Fast Skeletal Muscle Troponin Activator CK-2066260 Increases Fatigue Resistance by Reducing the Energetic Cost of Muscle Contraction," *Journal of Physiology* 597, no. 17 (2019): 4615–4625.

27. D. L. Arnold, P. M. Matthews, and G. K. Radda, "Metabolic Recovery After Exercise and the Assessment of Mitochondrial Function In Vivo in Human Skeletal Muscle by Means of ^{31}P NMR," *Magnetic Resonance in Medicine* 1 (1984): 307–315.

28. A. L. Basse, M. Agerholm, J. Farup, et al., "Nampt Controls Skeletal Muscle Development by Maintaining Ca^{2+} Homeostasis and Mitochondrial Integrity," *Molecular Metabolism* 53 (2021): 101271.

29. E. Palma, T. Tiepolo, A. Angelin, et al., "Genetic Ablation of Cyclophilin D Rescues Mitochondrial Defects and Prevents Muscle Apoptosis in Collagen VI Myopathic Mice," *Human Molecular Genetics* 18, no. 11 (2009): 2024–2031.

30. A. Zulian, E. Rizzo, M. Schiavone, et al., "NIM811, a Cyclophilin Inhibitor Without Immunosuppressive Activity, Is Beneficial in Collagen VI Congenital Muscular Dystrophy Models," *Human Molecular Genetics* 23, no. 20 (2014): 5353–5363.

31. W. A. Irwin, N. Bergamin, P. Sabatelli, et al., "Mitochondrial Dysfunction and Apoptosis in Myopathic Mice With Collagen VI Deficiency," *Nature Genetics* 35, no. 4 (2003): 367–371.

32. D. P. Millay, M. A. Sargent, H. Osinska, et al., "Genetic and Pharmacologic Inhibition of Mitochondrial-Dependent Necrosis Attenuates Muscular Dystrophy," *Nature Medicine* 14, no. 4 (2008): 442–447.

33. L. Merlini, A. Angelin, T. Tiepolo, et al., "Cyclosporin A Corrects Mitochondrial Dysfunction and Muscle Apoptosis in Patients With Collagen VI Myopathies," *Proceedings of the National Academy of Sciences* 105, no. 13 (2008): 5225–5229.

34. P. S. Brookes, Y. Yoon, J. L. Robotham, M. W. Anders, and S. S. Sheu, "Calcium, ATP, and ROS: A Mitochondrial Love-Hate Triangle," *American Journal of Physiology. Cell Physiology* 287, no. 4 (2004): C817–C833.

35. M. R. Duchen, "Mitochondria and Ca^{2+} in Cell Physiology and Pathophysiology," *Cell Calcium* 28, no. 5–6 (2000): 339–348.

36. R. Rizzuto, D. De Stefani, A. Raffaello, and C. Mammucari, "Mitochondria as Sensors and Regulators of Calcium Signalling," *Nature Reviews. Molecular Cell Biology* 13, no. 9 (2012): 566–578.

Supporting Information

Additional supporting information can be found online in the Supporting Information section.